

Time-Resolved High-Frequency EPR Studies on Magnesium and Zinc Tetraphenylporphines in Their Lowest Excited Triplet States[†]

Seigo Yamauchi,* Katsuaki Takahashi, Saiful S. M. Islam, Yasunori Ohba, and Valery Tarasov[‡]

Institute of Multidisciplinary Research for Advanced Materials, Tohoku University, Katahira 2-1-1, Aoba-ku, Sendai 980-8577, Japan

Received: March 14, 2010; Revised Manuscript Received: May 19, 2010

The lowest excited triplet (T_1) states of magnesium and zinc tetraphenylporphines (MgTPP and ZnTPP) were studied by time-resolved (TR) high-frequency/high-field W-band electron paramagnetic resonance (hf-EPR) spectroscopy in rigid glasses at low temperatures. Inspections of the TR-hf-EPR spectra of the spin-polarized triplets revealed that the zero field splitting (ZFS) parameters, D and E , for MgTPP and ZnTPP triplets were nearly the same. At the same time, their g -tensors were found to be different. These results are interpreted quantitatively in terms of spin–orbit couplings (SOCs) and angular momenta among the excited states, giving a magnitude of SOC in the T_1 state of ZnTPP. For the first time, both the TR-hf-EPR spectra and corresponding time profiles were acquired on the ZnTPP's triplet at room temperature in liquid paraffin solution with the populations of the electron spin states being in Boltzmann equilibrium. Because of relatively fast paramagnetic relaxation in rotating triplet at room temperature, the spectra and time profiles were free from the effects of microwave saturation that allowed for the direct measurement of the absolute intersystem crossing ratios $P_x:P_y:P_z$ 0.085:0.085:0.83. All of these results have demonstrated advantages and new perspectives of the W-band EPR spectroscopy.

Introduction

There have been extensive studies on the lowest excited triplet (T_1) states of metallo-porphyrins (MPs) by means of various kinds of spectroscopes. Among the characteristics of the T_1 state, dynamic parameters of the triplet sublevels such as intersystem crossing (ISC) ratios P_i ($i = x, y, z$) from the excited singlet S_1 state and corresponding decay rate constants k_i and static parameters such as zero field splitting (ZFS) parameters (D and E) and the principal values g_i of the g -tensor of T_1 can be obtained by the electron paramagnetic resonance (EPR) spectroscopy.

For the phosphorescent triplets, the parameters P_i , k_i , D , and E had been obtained by zero-field optically detected magnetic resonance (zf-ODMR)^{1,2} technique. For the nonphosphorescent molecules, time-resolved EPR (TR-EPR) spectroscopy of the electron spin-polarized molecular triplets ($T_1^\#$) was found to be capable of obtaining the similar information. Moreover, characteristics of anisotropic magnetic interactions such as parameters of ZFS D and E and components of the triplet g -tensors were obtained in the T_1 states. During the last few decades, many spin-polarized triplets have been detected and analyzed extensively^{4–6} by this method in low-temperature glass matrices and even in liquid solutions at room temperature.³

Spin–orbit couplings (SOCs) of the T_1 triplet state with the higher excited electronic states are well-known to effect on the anisotropy of the electron spin interactions and populations P_x , P_y , and P_z of the $T_1^\#$ triplet T_x , T_y , and T_z spin states in many organic metal complexes. Therefore, the knowledge of the principal values of g -tensors and absolute populations is of

significant importance for an assignment of the mechanisms of the SOCs in the T_1 states. However, because of low resolution, a small anisotropy in the electron spin Zeeman interaction (g -tensor) cannot be observed discernibly by means of X-band ($\nu = 9$ GHz) EPR spectroscopy. Whatever the frequency of EPR spectrometer, only the relative ratio of the triplet sublevels' populations $P_x:P_y:P_z$ ($P_z < P_x, P_y$) other than the absolute values $P_x:P_y:P_z$ can be obtained from the electron spin-polarized spectra acquired just immediately after the laser pulse.

The problems originated from low spectral resolution of X-band EPR spectroscopy can be overcome by using the time-resolved high-frequency/high-field W-band ($\nu = 95$ GHz) EPR.⁷ We applied this technique to study the T_1 states of two metallo-porphyrins, magnesium (MgTPP) and zinc (ZnTPP) tetraphenylporphines. For MgTPP, only in a solid solution and only spin-polarized triplets could be detected by W-band TR-EPR spectroscopy. For ZnTPP, we have succeeded to observe the W-band TR-EPR spectra acquired on both the spin-polarized and equilibrium molecular triplets in solid and liquid solutions. The g anisotropy was determined by the computer simulation of the W-band TR-EPR spectra of spin-polarized triplets. The results were interpreted in terms of SOCs with the higher triplet states $^3d\pi^*$, $^3\pi d$, and/or $^3\pi\pi^*$ and compared with those of palladium-porphine (PdP)⁸ and yttrium-porphine (YP).⁹ Obtained magnitudes of SOC were used to discuss parameter D of ZnTPP triplet.

The absolute ISC ratios $P_x:P_y:P_z$ of the triplet T_x , T_y , and T_z electron spin sublevels of the ZnTPP spin polarized triplet were obtained from the kinetic analysis of the room-temperature time profiles and compared with the value obtained by ODMR at very low temperatures.¹

Experimental Section

Synthesis and purification of ZnTPP and MgTPP have been previously described.¹⁰ Toluene (spectral grade) was purchased

[†] Part of the "Michael R. Wasielewski Festschrift".

* To whom correspondence should be addressed. Tel: +81-22-217-5617. Fax: +81-22-217-5616. E-mail: yamauchi@tagen.tohoku.ac.jp.

[‡] Present address: Institute of Chemical Physics, RAS, Kocygina St., Moscow 119991, Russia.

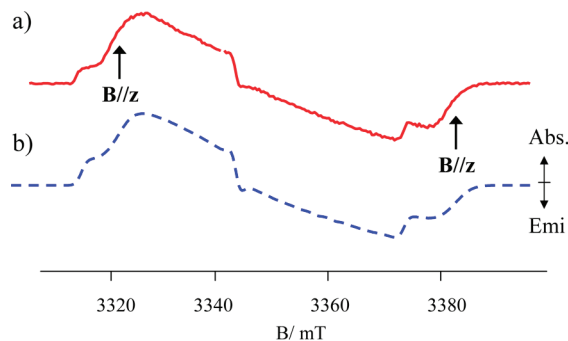


Figure 1. (a) Time-resolved W-band EPR spectrum of ZnTPP triplet state observed at 40 K and 1 μ s after the laser pulse in toluene and (b) its simulation. The stationary fields $B//z$ are indicated.

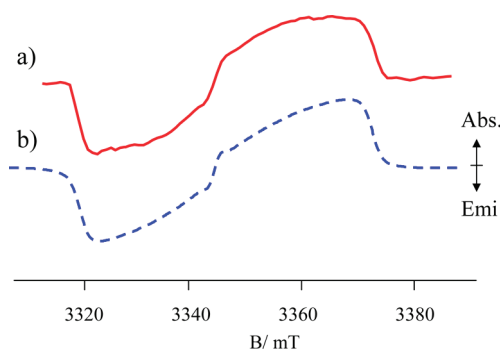


Figure 2. (a) Time-resolved W-band EPR spectrum of MgTPP triplet state observed at 40 K and 1 μ s after the laser pulse in toluene and (b) its simulation.

from Wako Chemical Co. and used as received. Toluene solutions (0.1 mM of ZnTPP or MgTPP) were deaerated by freeze–pump–thaw cycles and sealed under vacuum in a 0.8 mm (o.d.) quartz tube for the W-band EPR experiment.

A Bruker E-680 W-band EPR spectrometer was modified for higher time resolution and effective laser excitation in the TR-EPR experiment. A working microwave frequency was ~ 94.16 GHz. To get higher time resolution, the standard 6 MHz Bruker preamplifier was replaced with 140 MHz low-noise NF SF-230F5 amplifier, which improved the time resolution up to 5 ns. To reach the most optimum irradiation from Spectra Physics MOPO-SL OPO laser (550–610 nm) pumped by the third harmonic (355 nm) of a Spectra Physics PRO270–20 Nd/YAG laser, a light fiber of 0.5 mm diameter was inserted into the sample tube and put on just above the sample solution. The power of the laser was 2 to 3 mJ/pulse. Temperature (10–80 K) was controlled by an Oxford ER4112HV helium temperature cryosystem.

Results

Acquired at 100 ns time delay after the laser pulse, the TR EPR spectra of the ZnTPP and MgTPP triplets in low-temperature toluene glass are represented in Figures 1 and 2, respectively. Parameters used to simulate spectra are given in Table 1. The molecular structure, axes, and spin sublevel scheme are shown in Figure 3. The zero-field splitting parameters D and E and the relative populating ratio $P_x-P_y:P_z-P_y$ were taken from literature.^{7,10} Because it follows from the Table that the g_z values of MgTPP and ZnTPP are noticeably smaller than g_e ($= 2.0023$) with g_z of ZnTPP triplet being essentially smaller than that of MgTPP. Only minor deviations from g_e were observed for the g_x and g_y values in both triplets.

TABLE 1: EPR Parameters and Kinetic Parameters Used for Simulations of Time-Resolved EPR Spectra Observed at 40 K

	zero-field splitting		g value ^a		ISC ratio
	D/MHz	E/MHz	g_x, g_y	g_z	
ZnTPP	906	284	2.0020, 2.0024	1.9968	0:1
MgTPP	904	280	2.0022	2.0018	0.50:0.50 ^b

^a Errors in the g values are estimated to be ± 0.0003 . ^b Ratio of $P_x-P_z:P_y-P_z$ in ref 10.

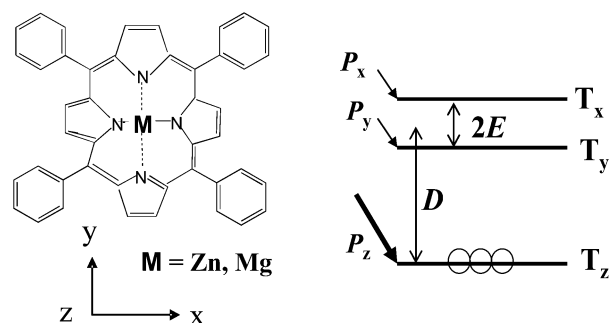


Figure 3. Molecular structures, axes, and triplet sublevel scheme.

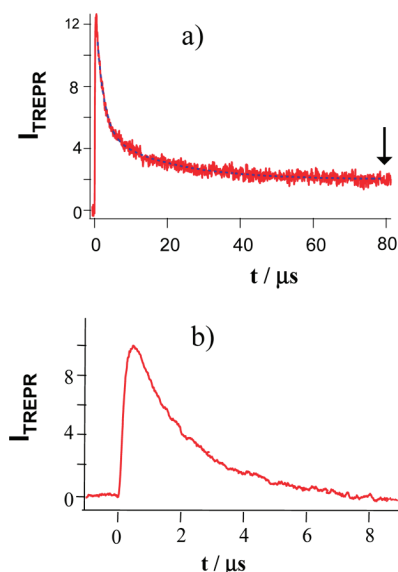


Figure 4. Time-profiles of (a) W-band and (b) X-band EPR signals of ZnTPP at $B//z$ in the low field side (Figure 5) at 40 K. The arrow indicates the time when the thermalized spectrum is observed in Figure 5.

A time profile of the EPR signal at 40 K and $B//z$ of the low field side is composed of the fast and slow components (Figure 4a). The fast decaying component comes from the usual spin polarization, as simulated in Figure 1. The decay curve in Figure 4a is very different from that observed at the X-band (Figure 4b), which could be fitted adequately by a single exponential function. We assign the W-band TR EPR spectrum (Figure 5, solid line) at longer time delays (>20 μ s) to the EPR spectrum of the ZnTPP spin-thermalized triplet state by comparing it with the simulated one (a dotted line in Figure 5). Consistency of the two spectra leaves something to be desired, probably because of effects of microwave saturation.

At room temperature in liquid paraffin solution, TREPR spectra from the spin-polarized (66 ns time delay) and spin-equilibrium (3.8 μ s time delay) ZnTPP triplet state are shown in Figure 6a,b, respectively (solid lines), together with their simulations (dashed lines). The E value was found to be virtually

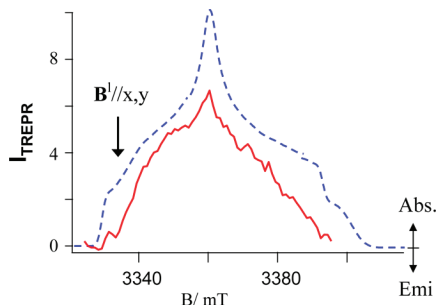


Figure 5. Time-resolved W-band EPR spectrum of ZnTPP observed at 40 K and 20 μ s after the laser pulse in toluene and its simulation (dotted line). The decay curve in Figure 4a was observed at the field B^l/z indicated by the arrow.

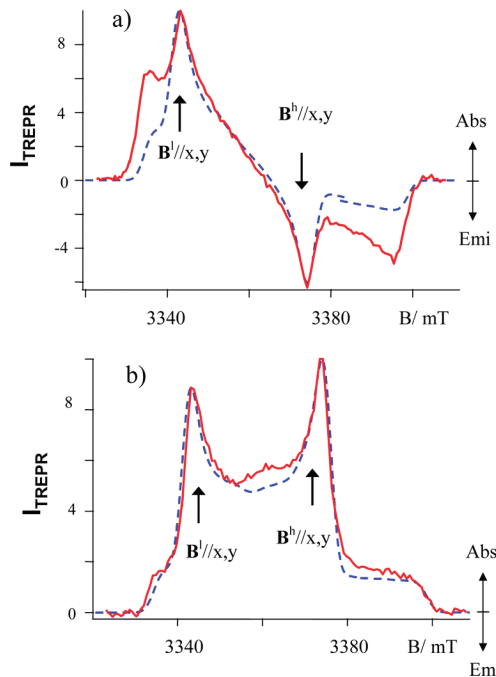


Figure 6. Time-resolved W-band EPR spectra of ZnTPP observed at (a) 50–80 ns and (b) 3.4 to 4.2 μ s after the laser pulse at room temperature. The spectral simulations are also shown by dotted lines.

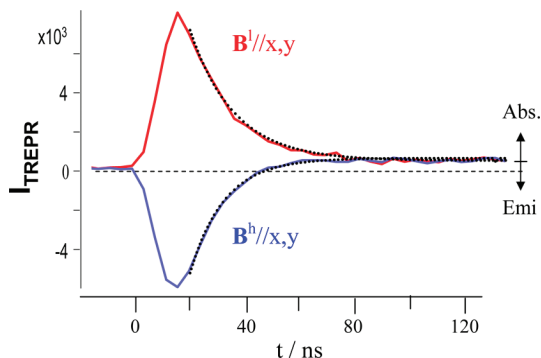


Figure 7. Time profiles of the W-band EPR signals of ZnTPP at the low field $B^l//x,y$ and high field $B^h//x,y$ sides. The dotted lines indicate decay curves simulated with eq 9 and the parameters summarized in Table 2.

nil ($E = 0$), indicating that fast interconversion occurs between the Jahn–Teller split T_1 and T_2 states.^{6,11}

The time profiles of the low- and high-field components the EPR signal taken at $B^l//x,y$ are labeled as $B^l//x,y$ and $B^h//x,y$ curves in Figure 7.

TABLE 2: Kinetic Parameters Used for Simulations of Decay Curves for EPR Signals of ZnTPP at Room Temperature

	$A_p(\text{rel})$	$A_t(\text{rel})$	A_p/A_t	k_p/s^{-1}	k_d/s^{-1}
I_{LF}	27 700	380	73	7.1×10^7	1.8×10^3
I_{HF}	−32 700	480	−68	8.5×10^7	1.8×10^3

Discussion

1. Interpretation of EPR Parameters. The zero-field splitting parameters D and E are nearly the same and only the g_z value varies with metal substitution from Mg to Zn, as shown in Table 1. We discuss these results in terms of SOC between $T_1(\pi\pi^*)$ and the higher excited triplet (T_2) states. The candidates for the T_2 state(s) are $d\pi^*$ states such as what happens with platinum (Pt) complex,¹² πd states, and the Jahn–Teller split $\pi\pi'^*$ state as in the cases of PdP⁸ and YOEP⁹ (OEP: octaethylporphyrine). The shift in g_z is given by¹³

$$\Delta g_z = g_e - g_z = -\frac{2\langle\psi_{T_1}(\pi\pi^*)|L^z|\psi_{T_2}\rangle\langle\psi_{T_2}|\lambda_M^z|\psi_{T_1}(\pi\pi^*)\rangle}{E(T_2) - E(\pi\pi^*)} \quad (1)$$

As it follows from eq 1, positive ($g_z > g_e$) and negative ($g_z < g_e$) shifts are expected for the case of the “electron (α -spin) excitation” and “hole (β -spin) excitation”,⁷ respectively. The perturbing higher $d\pi^*$ states correspond to the former, and the πd and $\pi\pi'^*$ states correspond to the latter. The experimentally observed negative shift ($g_z = 1.9968$) indicates that the $d\pi^*$ states are not involved in the case discussed. Because the central Zn (II) ion possesses d^{10} electrons, the πd state is also excluded from possible candidates. Then, the shift in the g_z value most likely comes from SOC with the Jahn–Teller split $\pi\pi'^*$ state.

For ZnTPP and MgTPP complexes,^{9,10} $T_1(\pi\pi^*)$ and $T_2(\pi\pi'^*)$ states belong to either ($a_{2u}e_{gx}$) or ($a_{2u}e_{gy}$) configurations. A possible origin of large SOC is a delocalization of the π^* electrons over the porphyrin ring (e_{gx}^0 and e_{gy}^0) and π -type d_{zx} and d_{yz} orbitals of the central metal ion, as described by eqs 2a

$$e_{gx} = C_x e_{gx}^0 + C_{zx} d_{zx} \quad (2a)$$

$$e_{gy} = C_y e_{gy}^0 + C_{yz} d_{yz} \quad (2b)$$

The e_{gx}^0 and e_{gy}^0 orbitals are nearly degenerate LUMO orbitals of TPP. On the basis of this model, contributions of SOC to D and g_z can be described by eqs 3 and 4.^{8,9}

$$D_{SO} = Z'^2/4\Delta E_{TT} \quad (3)$$

$$\Delta g_z = g_e - g_z = Z'\Lambda'/\Delta E_{TT} \quad (4)$$

The necessary parameters are defined by eqs 5–7

$$iZ' = iZq = C_{zx}C_{yz}\langle d_{yz}|\hat{L}_z|d_{zx}\rangle\langle\varphi(T_1)|\varphi(T_2)\rangle \quad (5)$$

$$\Delta E_{\text{TT}} = E(T_2) - E(T_1) \quad (6)$$

$$i\Lambda' = i\Lambda\Lambda = C_{zx}C_{yz}\langle\psi(T_1)|l_z|\psi(T_2)\rangle\langle\varphi(T_1)|\varphi(T_2)\rangle \quad (7)$$

It follows from the equations above that

$$D_{\text{SO}}/\Delta g_{zz} = Z'/4\Lambda' = Z/4\Lambda \quad (8)$$

To estimate Λ' ($= 1.8$) and q ($= 0.58$), we average corresponding values for PdP (respectively, 1.5 and 0.63)⁸ and YOEP (2.1 and 0.52).⁹ The validity of Λ' comes from similarity for Λ' values of ZnTPP and PdP in the S_1 states.¹⁴ The q value, an overlap integral of the vibrational wave functions of T_1 and T_2 (eqs 5 and 7), should reflect the magnitude of ΔE_{TT} , which is 110 and 114 cm^{-1} for ZnTPP⁶ and YOEP,⁹ respectively. Then, we obtain Z' as 0.34 cm^{-1} from $\Delta g_z (= 2.0023 - 1.9968 = 0.0055)$ and eq 4. D_{SO} is evaluated as 7.9 MHz from Z , ΔE_{TT} , and eq 3 and is consistent with the obtained D values (≤ 10 MHz) of ZnTPP (906 MHz) and MgTPP (904 MHz).

On the basis of the Z' value, we can calculate Z to be 0.59 ($= 0.34/0.58$) cm^{-1} from eq 5 and determine $C_{zx}C_{yz}$ as 0.0015 from $\nu_{\text{Zn}} = 386 \text{ cm}^{-1}$ ¹⁵ and eq 5. If we postulate that $C_{zx} = C_{yz}$, then 3.9% of π -electrons are found to delocalize over the Zn atom. A much smaller shift in g_z is expected for MgTPP based on $\nu_{\text{Mg}} = 41 \text{ cm}^{-1}$ ¹⁶ and was observed as $\Delta g_z = 0.0006$ (cf. 0.0055 for ZnTPP).

For a sign of the g shift, the important perturbing $T_2(\pi\pi^*)$ state corresponds to the “ $\pi^* \rightarrow \pi^*$ electron excitation” with respect to the $T_1(\pi\pi^*)$ state. In this case, $\lambda_{\text{M}} = +\zeta_{\text{M}}$ (SOC parameter of M) and λ_{M} becomes positive in eq 1, providing a negative shift ($\Delta g_z < g_e$), as observed.

2. Absolute Intersystem Crossing Ratio. From the TREPR experiment, we can obtain only the relative ISC ratio $P_x:P_z:P_y$ ($P_z < P_x, P_y$). This ratio does not help much when one needs to determine the absolute populations because the sets $P_x:P_y:P_z = 0:0:1$ and $0.33:0.33:0.34$ give the same values $P_x:P_y:P_z = 0:1$. If we were able to observe a TREPR spectrum from the equilibrium triplet, we could obtain the absolute populations in the spin-polarized triplet state because the absolute populations in the spin equilibrium triplet can be calculated accurately for any orientation of the triplet in the magnetic field of the spectrometer. Observation of the TR EPR spectra at the very long delay times meets two main difficulties. One is a small amount of paramagnetic centers. The other is the influence of the resonance microwave field on the spectral shape. To avoid effects of microwave saturations, one needs to use very weak microwave fields, inevitably losing the sensitivity. Fortunately, this is not necessary to possess the spectrum; accurate measurement of the EPR signal intensity in a particular magnetic field is quite enough to obtain the desired result. Now one can simply increase the number of scans to obtain better S/N ratio without dramatic increase in experimental time. Moreover, this is quite enough to simulate successfully only one spectrum acquired on either the spin-polarized or spin-equilibrium triplet because the parameters of the relevant spin Hamiltonian can confidently be used to calculate the necessary Boltzmann populations.

It is worthwhile to note that the intensities of thermalized signals at W-band EPR increase by a factor of 10 as compared with those at the X-band. This is why we failed to observe TR-EPR of the equilibrium triplets using X-band EPR spectroscopy.

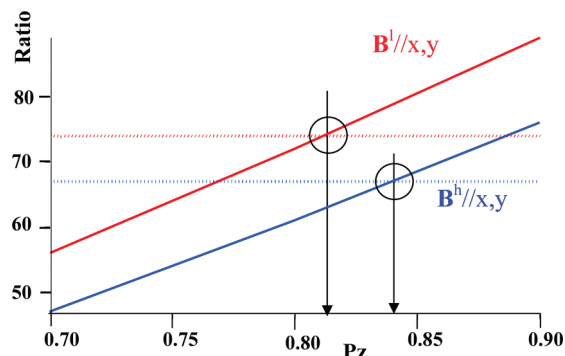


Figure 8. Calculations of the ratio of EPR signals at $t = 0$, A_p/A_t for each P_z value at low and high stationary fields, $B^l/x,y$ and $B^h/x,y$. The P_z value is determined from the obtained A_p/A_t values, as indicated in the figure.

In the case of ZnTPP in liquid paraffin, both polarized and thermalized spectra were reasonably consistent with the simulated ones. For the time delays $t_{\text{obsd}} > 30$ ns, the time profiles can be fitted by two exponential functions

$$I(t) = A_p \exp(-k_p t) + A_t \exp(-k_t t) \quad (9)$$

One represents the fast kinetics, and the other represents the slow kinetics. Slow kinetics with the rate constant k_t ca. $9 \times 10^4 \text{ s}^{-1}$ is likely to be due to decay of the spin equilibrium triplet due to radiating, nonradiating, and chemical decay processes. Indexes “p” and “t” denote the polarized and thermalized components, respectively. The fast component represents the relaxation of the spin populations in spin-polarized triplet.

The analyses of the decay curves in Figure 7 and those within a wider time range provided the pre-exponential factors A_p and A_t and the decay rate constants k_p and k_t , as summarized in Table 2. The k_t and k_p values give rise to a triplet lifetime of 560 μs and a spin population’s relaxation time of 12–14 ns for ZnTPP in liquid paraffin at room temperature. The pre-exponential factors, A_p and A_t , are used to evaluate the magnitude of spin polarization in the ISC process. When we refer to the simulated spectra in Figure 6, we can calculate the relative value of A_p/A_t for each P_z value at both the low and high stationary fields of $B^l/x,y$ as shown in Figure 8. From the obtained ratio of A_p/A_t (Table 2), 73 at $B^l/x,y$ and 68 at $B^h/x,y$ shown by dotted lines in Figure 8, $P_z = 0.81$ and 0.84 are obtained, respectively. Finally, the absolute ISC ratio is determined to be $P_x:P_y:P_z = 0.085:0.085:0.83$ with an accuracy of $P_z = 0.81$ to 0.84 at room temperature. This ratio is compared with that (0.03:0.03:0.94) obtained by ODMR for ZnP in *n*-octane at 1.3 K.¹⁶ The difference must come from higher mobility of the molecule in liquid solution.⁶ Therefore, to determine the ISC ratio of the triplet sublevels, this method was demonstrated to be unique and informative.

The fact that at low temperatures such as 40 K, the spectrum from the equilibrium triplet cannot be simulated well, as shown in Figure 5, is not of crucial importance because the spectra of polarized triplets could be simulated perfectly indeed. However, the similar treatments of time profiles taken at different magnetic fields result in rather wide scatter in values of absolute populations. This is probably due to microwave saturation, which is not easy to remove because the evolution of spectra takes milliseconds. Spin-selectivity of triplet decay into the ground singlet state could also be a disturbing factor.

The thermalized component of net absorption was not observed for MgTPP. We examined a pulsed microwave

W-band EPR experiment and have obtained preliminary results for the thermalized component of ZnTPP, which seem to be free from saturation. We will report on these analyses in a forthcoming paper.

Acknowledgment. This work was supported by Grant-in-Aid for Scientific Researches nos. 19350003 and 21655003 from the Ministry of Education, Science, Culture, and Sports, Japan.

References and Notes

- (1) (a) Scharnoff, M. J. *Chem. Phys.* **1967**, *46*, 3263–3264. (b) Kwiram, A. L. *Chem. Phys. Lett.* **1967**, *1*, 272–275. (c) Schmidt, J.; Hesselmann, I. A.; van der Waals, J. H. *Chem. Phys. Lett.* **1967**, *1*, 434–436.
- (2) Connors, R. E.; Leenstra, W. R. In *Triplet State ODMR Spectroscopy*; Clarke, R. H., Ed; John Wiley & Sons: New York, 1982; pp 257–289.
- (3) Fujisawa, J.; Ohba, Y.; Yamauchi, S. *J. Am. Chem. Soc.* **1997**, *119*, 8736–8737.
- (4) Hirota, N.; Yamauchi, S. *Dynamics of Excited Molecules*; Kuchitsu, K., Ed.; Elsevier: Amsterdam, 1994; pp 513–557.
- (5) Murai, H.; Tero-Kubota, S.; Yamauchi, S. *Specialist Periodical Reports: Electron Spin Resonance*; The Royal Society of Chemistry: Cambridge, U.K., 2000; Vol. 17, pp 130–163.
- (6) Yamauchi, S. *Bull. Chem. Soc. Jpn.* **2004**, *77*, 1255–1268.
- (7) Yamauchi, S.; Tanabe, M.; Takahashi, K.; Islam, S.; Matsuoka, H.; Ohba, Y. *Appl. Magn. Reson.* **2010**, *37*, 317–323.
- (8) Kooter, J. A.; Canters, G. W.; van der Waals, J. H. *Mol. Phys.* **1977**, *33*, 1545–1563.
- (9) Ishii, K.; Ohba, Y.; Iwaizumi, M.; Yamauchi, S. *J. Phys. Chem.* **1996**, *100*, 3839–3846.
- (10) Yamauchi, S.; Matsukawa, Y.; Ohba, Y.; Iwaizumi, M. *Inorg. Chem.* **1996**, *35*, 2910–2914.
- (11) Fujisawa, J.; Ishii, K.; Ohba, Y.; Iwaizumi, M.; Yamauchi, S. *J. Phys. Chem.* **1995**, *99*, 17082–17084.
- (12) Funayama, F.; Kato, M.; Kosugi, H.; Yagi, M.; Higuchi, J.; Yamauchi, S. *Bull. Chem. Soc. Jpn.* **2000**, *73*, 1541–1550.
- (13) Stone, A. J. *Proc. R. Soc. London* **1963**, *A205*, 424–434.
- (14) (a) Canter, G. W.; van der Waals, J. H. In *The Porphyrins*; Dolphin, D., Ed.; Academic Press: New York, 1978; Vol. III, pp 531–582. (b) Gouterman, M. *Ann. N. Y. Acad. Sci.* **1973**, *206*, 70–83.
- (15) Tripathy, U.; Kowalska, D.; Liu, X.; Velate, S.; Steer, R. P. *J. Phys. Chem. A* **2008**, *112*, 5824–5833.
- (16) Chan, I. Y.; van Dorp, W. G.; Schaafsma, T. J.; van der Waals, J. H. *Mol. Phys.* **1971**, *22*, 741–752; 753–760.

JP1023197